Journal of ELECTRONIC MATERIALS, Vol. 47, No. 6, 2018
https://doi.org/10.1007/s11664-017-6020-9

TOPICAL COLLECTION: INTERNATIONAL CONFERENCE ON THERMOELECTRICS 2017

High-Throughput Screening of Sulfide Thermoelectric Materials Using Electron Transport Calculations with OpenMX and BoltzTraP

MASANOBU MIYATA,[1,4] TAISUKE OZAKI,[2] TSUNEHIRO TAKEUCHI,[3] SHUNSUKE NISHINO,[3] MANABU INUKAI,[3] and MIKIO KOYANO[1]

1.—School of Materials Science, Japan Advanced Institute of Science and Technology, Ishikawa 923-1292, Japan. 2.—Institute for Solid State Physics, The University of Tokyo, Chiba 277-8581, Japan. 3.—Toyota Technological Institute, Nagoya 468-8511, Japan. 4.—e-mail: s1540016@jaist.ac.jp

The electron transport properties of 809 sulfides have been investigated using density functional theory (DFT) calculations in the relaxation time approximation, and a material design rule established for high-performance sulfide thermoelectric (TE) materials. Benchmark electron transport calculations were performed for $Cu_{12}Sb_4S_{13}$ and $Cu_{26}V_2Ge_6S_{32}$, revealing that the ratio of the scattering probability of electrons and phonons ($\kappa_{lat}\tau_{el}^{-1}$) was constant at about 2×10^{14} W K^{-1} m^{-1} s^{-1}. The calculated thermopower S dependence of the theoretical dimensionless figure of merit ZT_{DFT} of the 809 sulfides showed a maximum at 140 μV K^{-1} to 170 μV K^{-1}. Under the assumption of constant $\kappa_{lat}\tau_{el}^{-1}$ of 2×10^{14} W K^{-1} m^{-1} s^{-1} and constant group velocity v of electrons, a slope of the density of states of 8.6 states eV^{-2} to 10 states eV^{-2} is suitable for high-ZT sulfide TE materials. The Lorenz number L dependence of ZT_{DFT} for the 809 sulfides showed a maximum at L of approximately 2.45×10^{-8} V^2 K^{-2}. This result demonstrates that the potential of high-ZT sulfide materials is highest when the electron thermal conductivity κ_{el} of the symmetric band is equal to that of the asymmetric band.

Key words: Thermoelectric conversion, sulfides, DFT calculations, high-throughput screening

INTRODUCTION

Recently, thermoelectric (TE) technology, which can convert waste heat energy directly to electrical energy, has received attention to increase energy resources for society and mitigate global greenhouse effects.[1] TE materials can be evaluated using the figure of merit $ZT = S^2\sigma(\kappa_{el} + \kappa_{lat})^{-1}T$, where S is the thermopower, σ is the electrical conductivity, κ_{el} is the electronic thermal conductivity, κ_{lat} is the lattice thermal conductivity, and T is absolute temperature. Although tellurium compounds such as Bi_2Te_3 and PbTe are well known as conventional high-performance TE materials,[2,3] these materials include tellurium, which is rare and expensive. Environmentally friendly and cheap TE materials without Te must be used. This work specifically examined group 16 elements, and particularly sulfide TE materials, as alternatives to Te-based compounds, because sulfur is cheap, abundant, and environmentally friendly. Novel sulfide TE materials with high ZT values have been discovered in recent years using experimental methods.[4] Tetrahedrite-related materials show $ZT = 0.7$ at 665 K,[5] or $ZT = 0.95$ at 700 K.[6] Colusite $Cu_{26}V_2Ge_6S_{32}$ shows $ZT = 0.73$ at 663 K.[7] However, to confirm and accelerate discovery of higher-performance sulfide TE materials, it will be necessary to use computational as well as experimental methods.

(Received July 31, 2017; accepted December 9, 2017; published online December 21, 2017)

High-throughput screening of novel TE materials using first-principles calculations has received attention as computing performance has increased. Some candidate TE materials have already been identified using computational methods. LiZnSb with high ZT value of 2.0 was reported by Madsen,[8] while the electronic part of the TE properties of 48,000 stoichiometric inorganic compounds was reported by Chen et al.[9] Among binary compounds, ZnSb, CdSb, and ZnAs were screened by Gorai et al. using electron transport calculations.[10] Experimental and theoretical results for the novel TE material β-In_2S_3 (ZT = 0.53 at 700 K) were reported by Chen et al.[11] Nevertheless, computer-aided screening has rarely been used to investigate ternary or more complex, environmentally friendly sulfide compounds.

In the present work, electron transport calculations of 809 sulfides were performed directly using OpenMX[12,13] and BoltzTraP.[14] We investigated the TE properties of these 809 sulfides in the relaxation time approximation and established a material design rule for high-performance sulfide TE materials.

COMPUTATIONAL METHODS

First-principles electronic structure calculations were conducted using the OpenMX software package based on density functional theory (DFT), norm-conserving pseudopotentials, and pseudo-atomic localized basis functions. We adopted the generalized gradient approximation (GGA) exchange correction potential proposed by Perdew et al.[15] After obtaining the E–k relation, electron transport calculations (ETCs) were carried out using the BoltzTraP code based on Boltzmann theory. However, the format of the input file for BoltzTraP is unsupported by OpenMX. We therefore created an interface program to connect the file format of OpenMX to that of BoltzTraP using a shell script program. Benchmark ETCs for undoped Si and conventional half-Heusler compounds (ZrCoM, M = As, Sb, Bi) are presented in the Electronic Supplementary Material, showing good agreement with all-electron DFT calculations using the WIEN2k code[16] and BoltzTraP (see Supplementary Figs. S1, S2). We calculated the relative electrical conductivity $\sigma\tau_{el}^{-1}$, thermopower S, relative electronic thermal conductivity $\kappa_{el}\tau_{el}^{-1}$, and theoretical dimensionless figure of merit ZT_{DFT} at chemical potential μ according to the following equations:

$$K_n = \int \sigma(\varepsilon, T)(\varepsilon - \mu)^n \left(-\frac{\partial f_{FD}}{\partial \varepsilon}\right) d\varepsilon,$$

$$\sigma(T) = K_0, S(T) = -\frac{1}{|e|T}\frac{K_1}{K_0}, \kappa_{el}(T) = \frac{1}{|e|^2 T}\left(K_2 - \frac{K_1^2}{K_0}\right), \quad (1)$$

where K_n is the transport coefficient, $\sigma(\varepsilon, T)$ is the conductivity spectrum at ε and T, ε is the energy, μ is the chemical potential, f_{FD} is the Fermi–Dirac distribution function, e is the elementary electric charge, and T is absolute temperature.

For estimation of a suitable electron relaxation time τ_{el} and lattice thermal conductivity κ_{lat}, we performed benchmark ETCs of tetrahedrite $Cu_{12}Sb_4S_{13}$ and colusite $Cu_{26}V_2Ge_6S_{32}$, which are known as novel TE materials. ZT can be separated mathematically into two terms as follows:

$$ZT = \frac{S^2\sigma}{\kappa_{el}} T \cdot \frac{1}{1 + \frac{\kappa_{lat}}{\kappa_{el}}}, \quad (2)$$

where the first term $S^2\sigma T\kappa_{el}^{-1}$ is designated factor A, while the second term $(1 + \kappa_{lat}\kappa_{el}^{-1})^{-1}$ is designated as factor B. The A factor can be calculated using only DFT calculations for electrons. However, the B factor cannot be calculated using DFT calculations of electrons, because it includes τ_{el} and κ_{lat}. Here, κ_{lat} is described as

$$\kappa_{lat} = \frac{1}{3} C_{lat} v_{lat}^2 \tau_{lat}, \quad (3)$$

where C_{lat} is the specific heat of the lattice, v_{lat} is the phonon group velocity, and τ_{lat} is the phonon relaxation time. According to Eq. 3, $\kappa_{lat}\tau_{el}^{-1}$ can be described as follows:

$$\frac{\kappa_{lat}}{\tau_{lat}} = \frac{1}{3} C_{lat} v_{lat}^2 \frac{\tau_{lat}}{\tau_{el}}. \quad (4)$$

When C_{lat} and v_{lat} are constant, $\kappa_{lat}\tau_{el}^{-1}$ is proportional to $\tau_{lat}\tau_{el}^{-1}$, which indicates that the physical meaning of $\kappa_{lat}\tau_{el}^{-1}$ is the ratio of the scattering probabilities of electrons and phonons. For quantitative calculation of the theoretical dimensionless figure of merit ZT_{DFT}, $\kappa_{lat}\tau_{el}^{-1}$ is important.

We estimated τ_{el} and κ_{lat} for high-performance sulfide TE materials tetrahedrite $Cu_{12}Sb_4S_{13}$ and colusite $Cu_{26}V_2Ge_6S_{32}$ by comparison of experimentally obtained results[5,6] with calculation results. Subsequently, suitable $\kappa_{lat}\tau_{el}^{-1}$ was obtained for calculating ZT_{DFT}. The ZT_{DFT} values for conventional TE materials Bi_2Te_3, PbTe, SnSe,[17] $Cu_{12}Sb_4S_{13}$, and $Cu_{26}V_2Ge_6S_{32}$ were also calculated using OpenMX and BoltzTraP.

ETCs were performed for 809 sulfides, including stoichiometric compounds and substitutional systems. A list of the 809 sulfides investigated is presented in Table SII of the Appendix. The flowchart of the electron transport calculations for the 809 sulfides is depicted in Fig. 1. Crystal structure information for the stoichiometric sulfide compounds was obtained from the Material Project database.[18] The substitutional sulfide compound systems were obtained by substituting each site for other atoms. The lattice parameter of the primitive cell of the sulfides was calculated using

CIF2Cell software.[19] The reciprocal lattice vector and suitable mesh size in **k** space were calculated automatically. The input file for OpenMX was created using a program written specifically for this purpose. We adopted an electronic temperature of 673 K, used the GGA exchange correlation potential, and considered spin–orbit coupling. The pseudo-atomic orbital basis function for each element is presented in Table I, where the symbols respectively denote the element, the cutoff radius (unit in Bohr), and the specification of the optimized orbitals.[12] We adopted a mesh distance in **k** space of about 0.05 $bohr^{-1}$ $mesh^{-1}$ and an energy cutoff at 500 Ry in the numerical integrations to obtain the *E–k* dispersion relation. The internal atomic coordinates and lattice parameter were fully optimized until the maximum force became less than 0.0001 hartree $bohr^{-1}$ using the quasi-Newton method.[20–25] As initial parameters, we used the atomic coordination and lattice parameter in the Material Project database.[18]

RESULTS AND DISCUSSION

Estimation of Electron Relaxation Time τ_{el} and Lattice Thermal Conductivity κ_{lat}

For the benchmark ETCs on $Cu_{12}Sb_4S_{13}$ and $Cu_{26}V_2Ge_6S_{32}$, we estimated the relaxation time τ_{el} by comparison with the experimental electrical conductivity σ. We calculated the relative electrical conductivity $\sigma\tau_{el}^{-1}$. Subsequently, the lattice thermal conductivity κ_{lat} was calculated using the relation $\kappa_{lat} = \kappa_{total} - \kappa_{el}$, where κ_{total} is the experimental thermal conductivity. The calculation results for τ_{el}, κ_{lat}, and $\kappa_{lat}\tau_{el}^{-1}$ for $Cu_{12}Sb_4S_{13}$ and $Cu_{26}V_2Ge_6S_{32}$ are presented in Table II. The results indicate that κ_{lat} and τ_{el} respectively depend on the material. We estimated κ_{lat} and τ_{el} as 1 W K^{-1} m^{-1} and 5 fs, respectively, based on the intermediate value of the benchmark calculation results. However, the $\kappa_{lat}\tau_{el}^{-1}$ value for $Cu_{12}Sb_4S_{13}$ and $Cu_{26}V_2Ge_6S_{32}$ was constant at about 2×10^{14} W K^{-1} m^{-1} s^{-1}. This result supports our inference that a $\kappa_{lat}\tau_{el}^{-1}$ value of 2×10^{14} W K^{-1} m^{-1} s^{-1} is suitable for calculating *ZT* values of high-performance sulfide TE materials.

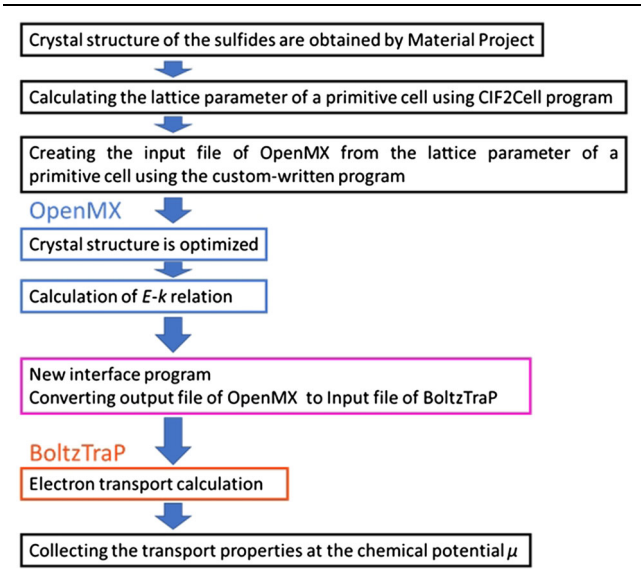

Fig. 1. Flowchart of electron transport calculations for 809 sulfides.

ZT_{DFT} Calculations for Conventional TE Materials

Using the constant values for κ_{lat} of 1 W K^{-1} m^{-1} and τ_{el} of 5 fs, we performed benchmark calculations of the ZT_{DFT} value for conventional TE materials. Figure 2 shows the chemical potential μ dependence of ZT_{DFT} for the *a*,*b*-axis and *c*-axis of Bi_2Te_3 at 300 K. The maximum ZT_{DFT} of Bi_2Te_3 with *a*, *b*-axis reached 0.28 (*n*-type) and 0.32 (*p*-type). These values are about one-third of the experimental *ZT* value of 0.8.[26] This result suggests that the $\kappa_{lat}\tau_{el}^{-1}$ value for Bi_2Te_3 is much lower than 2×10^{14} W K^{-1} m^{-1} s^{-1}.

Table I. Pseudo-atomic orbital basis functions for each element for ETCs of 809 sulfides

Element	Pseudo-atomic orbital basis functions
Al	Al7.0-s3p3d2
Si	Si7.0-s2p2d1
P	P7.0-s3p3d2f1
S	S7.0-s3p3d2f1
Ti	Ti7.0-s3p3d2
V	V6.0-s3p3d2
Cr	Cr6.0-s3p3d2
Mn	Mn6.0-s3p3d3
Fe	Fe6.0S-s2p2d1
Co	Co6.0S-s2p3d2f1
Ni	Ni6.0S-s3p3d2f1
Cu	Cu6.0S-s2p2d2
Zn	Zn6.0S-s2p2d2
Ga	Ga7.0-s2p2d2
Ge	Ge7.0-s3p3d3f2
Zr	Zr7.0-s3p2d2
Nb	Nb7.0-s3p2d2
Mo	Mo7.0-s3p2d2f1
Sn	Sn7.0-s2p2d3f1
Ta	Ta7.0-s3p2d2f1
W	W7.0-s3p2d2f1

Table II. Electron relaxation time τ_{el}, lattice thermal conductivity, and $\kappa_{lat}\tau_{el}^{-1}$ for $Cu_{12}Sb_4S_{13}$ and $Cu_{26}V_2Ge_6S_{32}$ at 673 K

Material	τ_{el} (fs)	κ_{lat} (W K^{-1} m^{-1})	$\kappa_{lat}\tau_{el}^{-1}$ (W K^{-1} m^{-1} s^{-1})
$Cu_{12}Sb_4S_{13}$	6.8	1.0	1.5×10^{14}
$Cu_{26}V_2Ge_6S_{32}$	2.4	0.49	2.1×10^{14}

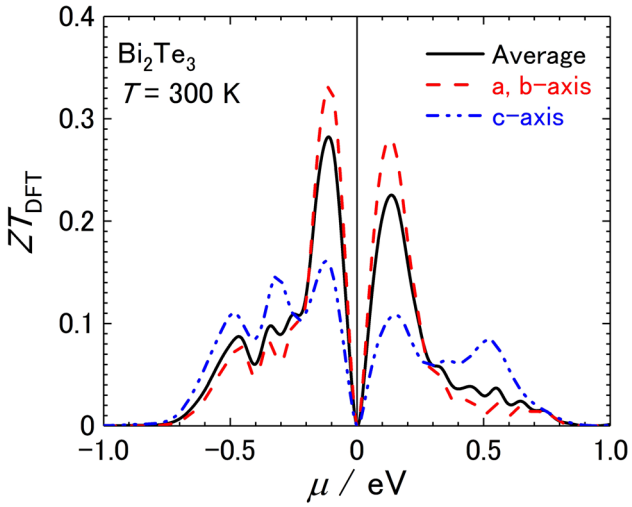

Fig. 2. Chemical potential μ dependence of ZT_{DFT} for Bi_2Te_3 at 300 K.

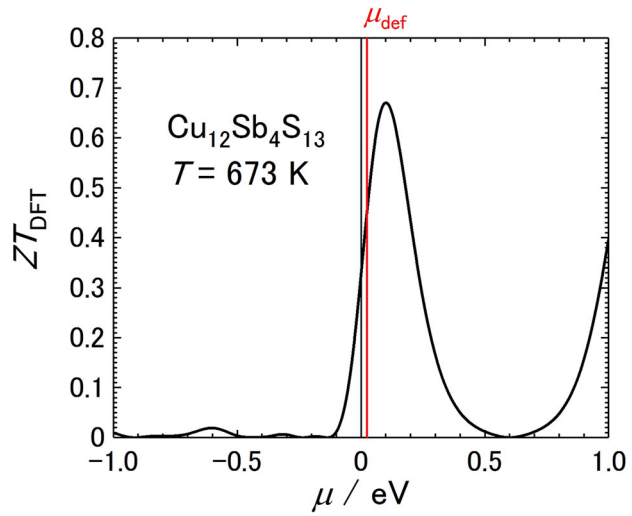

Fig. 3. Chemical potential μ dependence of ZT_{DFT} for $Cu_{12}Sb_4S_{13}$ at 673 K.

Figure 3 presents the μ dependence of ZT_{DFT} for tetrahedrite $Cu_{12}Sb_4S_{13}$ at 673 K. The value of ZT_{DFT} was 0.32 at μ, about two-thirds of the experimental ZT value of 0.5 found at 665 K.[5] This underestimation resulted from a difference in μ because the theoretical thermopower S was smaller than experimental values. We defined the location of μ_{def} to reproduce the experimental S. The ZT_{DFT} value at μ_{def} (red line) was 0.45 at 673 K, in good agreement with the experimentally obtained value. This result suggests that electron doping occurred in the experimental $Cu_{12}Sb_4S_{13}$ sample due to sulfur defects. The μ dependence of ZT_{DFT} for PbTe, SnSe, and $Cu_{26}V_2Ge_6S_{32}$ is not shown herein because their discussion is similar to that presented for Bi_2Te_3 or $Cu_{12}Sb_4S_{13}$.

Table III presents the maximum ZT_{DFT} value at $\mu \pm 0.5$ eV and the experimental ZT of Bi_2Te_3, PbTe, SnSe, $Cu_{12}Sb_4S_{13}$, and $Cu_{26}V_2Ge_6S_{32}$. The order of the maximum ZT_{DFT} value for $Cu_{12}Sb_4S_{13}$ and $Cu_{26}V_2Ge_6S_{32}$ is consistent with the experimental ZT. This result indicates that the $\kappa_{el}\tau_{el}^{-1}$ value of 2×10^{14} W K^{-1} m^{-1} s^{-1} is suitable for use with high-performance sulfide TE materials.

Electron Transport Calculations for 809 Sulfides

Figure 4 shows the thermopower S dependence of ZT_{DFT} at μ for the 809 sulfides at 673 K. Under the relaxation time approximation, the calculated ZT_{DFT} value increased concomitantly with increasing absolute value of S, showing maximum peaks at -170 μV K^{-1} (n-type) and 140 μV K^{-1} (p-type). Generally, high-performance TE materials require a sharp slope of the DOS under the assumption of constant τ_{el} and group velocity v of electrons. This guideline is known as the material design rule for high-performance TE materials. However, according to our calculation results, this guideline is incorrect. The S dependence of ZT_{DFT} in Fig. 4 shows that the suitable $|S|$ is 140 μV K^{-1} to 170 μV K^{-1}. Under the assumptions that τ_{el} and v are constant and that the DOS shows linear energy dependence, we can apply the expanded Mott formula as

$$|S| = \frac{\pi^2 k_B^2 T}{3|e|} \frac{1}{D(E_F)} \frac{\partial D(E_F)}{\partial E}, \quad (5)$$

where k_B is the Boltzmann constant, e is the elementary electric charge, E_F is the Fermi energy, $D(E_F)$ is the density of states at E_F, and E is the energy. When $|S|$ is 140 μV K^{-1} to 170 μV K^{-1} at 673 K, and when $D(E_F)$ is normalized as 1 state eV^{-1}, the calculated suitable slope of the DOS $\partial D(E_F)/\partial E$ at E_F is 8.6 states eV^{-2} to 10 states eV^{-2}.

To investigate the L dependence of ZT_{DFT} more deeply, we calculated the Lorenz number L dependence of the A factor ($= S^2\sigma T\kappa_{el}^{-1}$) and B factor ($= \{1 + \kappa_{lat}\kappa_{el}^{-1}\}^{-1}$). The A factor shows the L dependence, and increases with decreasing L. However, the B factor shows a maximum peak at the conventional Lorenz number $L_0 \sim 2.45 \times 10^{-8}$ V^2 K^{-2}. Figure 5 shows the L dependence of ZT_{DFT} ($= A$ factor $\times$ B factor) at 673 K. ZT_{DFT} increased concomitantly with increasing L, showing a maximum peak at $L_0 \sim 2.45 \times 10^{-8}$ V^2 K^{-2}. This result reflects that the contribution of the B factor is dominant. However, a small value of ZT_{DFT} was also found around L_0. This result indicates that some metallic systems show $L \sim L_0$, but the highest ZT materials show $L \sim L_0$; For example, the reported L of PbTe is 2.9×10^{-8} V^2 K^{-2} in the high-temperature region for maximizing ZT under consideration of multiband effects, as reported by Thesberg

Table III. Maximum ZT_{DFT} at $\mu \pm 0.5$ eV and experimental ZT of Bi_2Te_3, PbTe, SnSe, $Cu_{12}Sb_4S_{13}$, and $Cu_{26}V_2Ge_6S_{32}$

Materials	Maximum ZT_{DFT} at $\mu \pm 0.5$ eV	Experimental ZT
Bi_2Te_3 (a, b-axis, 300 K)	0.32 (p-type), 0.28 (n-type)	0.8[26]
PbTe (673 K)	1.6 (p-type)	1.2[28]
SnSe (*Pnma*, b-axis, 673 K)	0.9	0.6[29]
SnSe (*Cmcm*, b-axis, 923 K)	1.5	2.6 ± 0.3[29]
$Cu_{12}Sb_4S_{13}$ (673 K)	0.7	0.5 (665 K)[5]
$Cu_{26}V_2Ge_6S_{32}$ (673 K)	0.8	0.73 (665 K)[7]

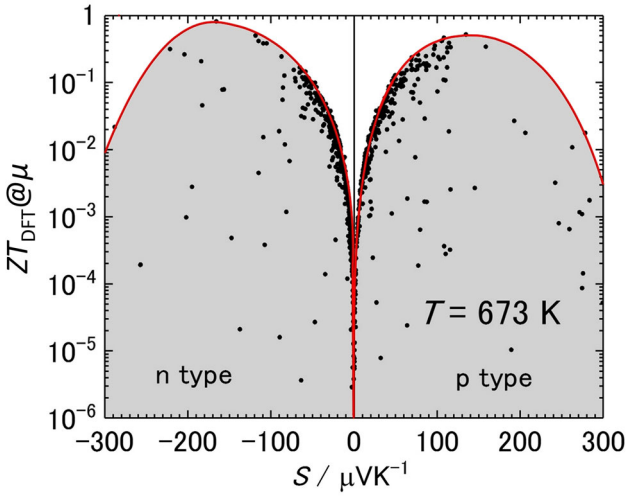

Fig. 4. Thermopower S dependence of ZT_{DFT} at μ for 809 sulfides at 673 K.

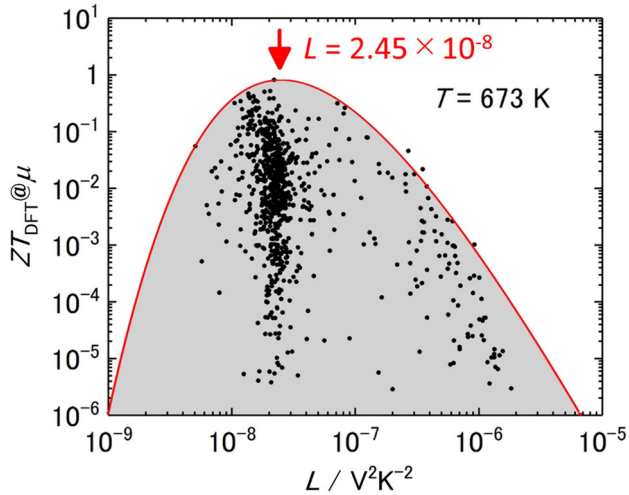

Fig. 5. Lorenz number L dependence of ZT_{DFT} at μ for 809 sulfides at 673 K.

et al.,[27] which supports our calculation results. Generally, $L = L_0$ is known as the degenerate limit. However, some sulfide materials in Fig. 5 show 10 to 100 times larger L values compared with L_0. The μ values of these materials are in the bipolar conduction region. Their bandgap is wide. For a two-band model in a bipolar system, the value of L is orders of magnitude larger. The maximum L increases concomitantly with increasing bandgap.[27] Also, κ_{el} is described as

$$\kappa_{el} = L_0 \sigma T + \frac{1}{|e|^2 T}(A - B), \tag{6}$$

$$A = \int \left\{ \sum_{n=1} \frac{1}{(2n)!} \sigma^{(2n)}(\mu, T)(\varepsilon - \mu)^{2n} \right\} (\varepsilon - \mu)^2 \left(-\frac{\partial f}{\partial \varepsilon} \right) \mathrm{d}\varepsilon, \tag{7}$$

$$B = \frac{\left[\int \left\{ \sum_{m=1} \frac{1}{(2m-1)!} \sigma^{(2m-1)}(\mu, T)(\varepsilon - \mu)^{2m-1} \right\} (\varepsilon - \mu) \left(-\frac{\partial f}{\partial \varepsilon} \right) \mathrm{d}\varepsilon \right]^2}{\int \left\{ \sum_{n=0} \frac{1}{(2n)!} \sigma^{(2n)}(\mu, T)(\varepsilon - \mu)^{2n} \right\} \left(-\frac{\partial f}{\partial \varepsilon} \right) \mathrm{d}\varepsilon}, \tag{8}$$

where L_0 is the conventional Lorenz number of 2.45×10^{-8} V^2 K^{-2}. According to these equations, A depends on the symmetric band around μ. The contribution of the asymmetric band is dominant in B. When $L = L_0$, the absolute values of A and B are expected to be equal. This result indicates that the κ_{el} of the symmetric band is equal to that of the asymmetric band when the potential for use as high-ZT materials is high.

CONCLUSIONS

We investigated the electron transport properties of 809 sulfides using density functional theory (DFT) calculations in the relaxation time approximation, and established a material design rule for high-performance sulfide TE materials.

In the benchmark calculations for $Cu_{12}Sb_4S_{13}$ and $Cu_{26}V_2Ge_6S_{32}$, the ratio of the scattering probability of electrons and phonons ($\kappa_{lat}\tau_{el}^{-1}$) was constant at about 2×10^{14} W K^{-1} m^{-1} s^{-1}. This value is suitable for calculation of the theoretical dimensionless figure of merit ZT_{DFT} of high-performance sulfide TE materials.

The calculated thermopower S dependence of ZT_{DFT} showed a maximum value at 140 μV K^{-1} to

170 μV K^{-1}. Under the assumption of constant $\kappa_{lat}\tau_{el}^{-1}$ of 2×10^{14} W K^{-1} m^{-1} s^{-1} and constant group velocity v of electrons, a slope of the DOS of 8.6 states eV^{-2} to 10 states eV^{-2} is suitable for high-ZT sulfide TE materials.

The Lorenz number L dependence of ZT_{DFT} showed a maximum value at around L of 2.45×10^{-8} V^2 K^{-2}. This result shows that the potential for high-ZT material is highest when the electronic thermal conductivity κ_{el} of the symmetric band is equal to that of the asymmetric band.

ACKNOWLEDGEMENTS

We are grateful to Dr. Toyoda (Industrial Research Institute of Ishikawa) for fruitful discussions related to thermoelectrics and physics. This work was supported financially by Grants from the Murata Science Foundation and the Thermoelectric Society of Japan, and by a JAIST Research Grant.

ELECTRONIC SUPPLEMENTARY MATERIAL

The online version of this article (https://doi.org/10.1007/s11664-017-6020-9) contains supplementary material, which is available to authorized users.

REFERENCES

1. L.E. Bell, *Science* 321, 1457 (2008).
2. O. Yamashita and S. Tomiyoshi, *J. Appl. Phys.* 95, 161 (2004).
3. J.P. Heremans, V. Jovovic, E.S. Toberer, A. Saramat, K. Kurosaki, A. Charoenphakdee, S. Yamanaka, and G.J. Snyder, *Science* 321, 554 (2008).
4. K. Suekuni and T. Takabatake, *APL Mater.* 4, 104503 (2016).
5. K. Suekuni, K. Tsuruta, M. Kunii, H. Nishiate, E. Nishibori, S. Maki, M. Ohta, A. Yamamoto, and M. Koyano, *J. Appl. Phys.* 113, 043712 (2013).
6. X. Lu, D.T. Morelli, Y. Xia, F. Zhou, V. Ozolins, H. Chi, X.Y. Zhou, and C. Uher, *Adv. Energy Mater.* 3, 342 (2013).
7. K. Suekuni, F.S. Kim, H. Nishiate, M. Ohta, H.I. Tanaka, and T. Takabatake, *Appl. Phys. Lett.* 105, 132107 (2014).
8. G.K.H. Madsen, *J. Am. Chem. Soc.* 128, 12140–12146 (2006).
9. W. Chen, J.H. Pöhls, G. Hautier, D. Broberg, S. Bajaj, U. Aydemir, Z.M. Gibbs, H. Zhu, M. Asta, G.J. Snyder, B. Meredig, M.A. White, K. Persson, and A. Jain, *J. Mater. Chem. C* 4, 4414–4426 (2016).
10. P. Gorai, P. Parilla, E.S. Toberer, and V. Stevanovic, *Chem. Mater.* 27, 6213–6221 (2015).
11. Y.X. Chen, A. Yamamoto, and T. Takeuchi, *J. Alloys Compd.* 695, 1631–1636 (2017).
12. T. Ozaki, *Phys. Rev. B* 67, 155108 (2003).
13. T. Ozaki and H. Kino, *Phys. Rev. B* 72, 045121 (2005).
14. G.K.H. Madsen and D.J. Singh, *Comput. Phys. Commun.* 175, 67–71 (2006).
15. J.P. Perdew, K. Burke, and M. Ernzerhof, *Phys. Rev. Lett.* 77, 3865 (1996).
16. P. Blaha, K. Schwarz, G.K.H. Madsen, D. Kvasnicka, J. Luitz, and WIEN 2K, *An Augmented Plane Wave + Local Orbitals Program for Calculating Crystal Properties*, ed. K. Schwarz (Wien: Techn. Universitat, 2001),.
17. G. Ding, G. Gao, and K. Yao, *Sci. Rep.* 5, 9567 (2015).
18. A. Jain, S.P. Ong, G. Hautier, W. Chen, W.D. Richards, S. Dacek, S. Cholia, D. Gunter, D. Skinner, G. Ceder, and K.A. Persson, *APL Mater.* 1, 011002 (2013).
19. T. Björkman, *Comput. Phys. Commun.* 182, 1183–1186 (2011).
20. C.G. Broyden, *J. Inst. Math. Appl.* 6, 76 (1970).
21. R. Fletcher, *Comput. J.* 13, 317 (1970).
22. D. Goldfarb, *Math. Comp.* 24, 23 (1970).
23. D.F. Shanno, *Math. Comp.* 24, 647 (1970).
24. A. Banerjee, N. Adams, J. Simons, and R. Shepard, *J. Phys. Chem.* 89, 52 (1985).
25. P. Csaszar and P. Pulay, *J. Mol. Struct. (Theochem.)* 114, 31 (1984).
26. T.M. Tritt, *Science* 283, 804 (1999).
27. M. Thesberg and H. Kosina, *Phys. Rev. B* 95, 125206 (2017).
28. S.N. Girard, J. He, X. Zhou, D. Shoemaker, C.M. Jaworski, C. Uher, V.P. Dravid, J.P. Heremans, and M.G. Kanatzidis, *J. Am. Chem. Soc.* 133, 16588–16597 (2011).
29. L.D. Zhao, S.H. Lo, Y. Zhang, H. Sun, G. Tan, C. Uher, C. Wolverton, V.P. Dravid, and M.G. Kanatzidis, *Nature* 508, 373–377 (2014).